Polish Society of Composite Materials
Polskie Towarzystwo Materiałów Kompozytowych

23: 1 (2023) 22-29

COMPOSITES THEORY AND PRACTICE
ISSN: 2084-6096
ISSN (online): 2299-128X

**Mateusz Kozioł**

*Silesian University of Technology, Faculty of Materials Engineering, ul. Z. Krasińskiego 8, 40-019 Katowice, Poland*
*Corresponding author. E-mail: mateusz.koziol@polsl.pl*

*Received (Otrzymano) 26.02.2023*

# EFFECT OF STRAIN RATE ON STATIC ELASTIC RESPONSE OF GLASS-POLYESTER COMPOSITE. PART 1: DESCRIPTION OF TEST METHOD

**This paper is the first of two parts of a pioneering study to evaluate the effect of the strain rate of a GFRP laminate on the stress response. The assessment concerns the elastic range of deformation only. The publication contains the assumptions and methodological description of the conducted experiments. The non-destructive bending tests and the methodology for determining the modulus of elasticity and the energy of the load-unload cycle are presented in detail. The full set of test results is presented in the appendix. The results and conclusions are discussed in the second part of the study, which is a separate publication.**

**Keywords: glass-polyester laminate, static bending, strain rate, normal stress, elastic modulus in bending, energy dissipation**

## INTRODUCTION

The strain rate of the material affects the intensity of its mechanical response. This effect is well known and studied for ranges of plastic deformation, especially in metals (the optimization of a rate of various plastic working processes is one of the most important issues in this field of technology [1, 2]). The growth in the stress in the material with the increase in the strain rate is basically explained by the intensification of flow (internal friction). In the case of metals, they are mutual displacements of crystal fragments, mainly in dislocation areas [2, 3]. In the case of polymeric materials, they are widely understood conformational movements of polymer chain segments, different for different types of polymers [4-6]. In the elastic range, the deformation of the material is mainly due to the straining of chemical (or physical) bonds, which is a reversible process [5, 7]. Theoretically, the elastic deformation of a material depends only on the amount of strain.

There is no good theoretical evidence to justify the rise in stress with the increase in the strain rate of the material in the elastic range. However, in the literature one can find publications containing test results indicating a clear influence of the strain rate on the stress response of materials in the elastic range. They are not very numerous, but Refs. [8] and [9] can be cited as examples. Reference [8] concerns brittle ceramic structures. It presents the overall results of the tests, including the elastic part and the development of failure. In all the analyzed cases, an evident increment in the energy utilized by the deformed element and a general increase in the stress level throughout the course of the tests (also within the elastic range) was found, along with growth in the strain rate. Reference [9] concerns steel. It was found that an increase in strain rate causes a rise in stress near the yield point. The yield strength grew by approx. 70 MPa with an increase in the strain rate from $10^{-3}$/s to $10^{2}$/s. Above this value, there is a further, very intensive increment in stress at the yield point with an increase in the strain rate – it should be emphasized that they are rather ballistic conditions. Also in Ref. [1], an evident (for some materials even more than 100%) rise in stress at the yield point of steel for the strain rate of $10^{2}$/s was found, compared to static conditions (not specified in the Ref. [1]).

In the available literature, it is impossible to find publications on the analysis of the effect of the strain rate on stress for FRP laminates, in particular those relating to the elastic range. This was the motivation to undertake preliminary studies in this direction. These studies have mainly a cognitive purpose, but important practical goals can be indicated in the case of further continuation of the work. Understanding the impact of the strain rate can contribute, e.g. to establishing new guidelines for the design of structures exposed to loads of varying speed (e.g. protective elements in the military industry), not only in the field of energy management during destruction, but also in order to make the structure resistant to the occurrence of irreversible dam-

age. It can be expected that FRP composites will exhibit behaviors that combine the features of elastic fibers and viscoelastic cured resins [10, 11]. The analyzed issue should not be combined with tests in dynamic-cyclic conditions (DMA tests). Such tests do not always take into account the behavior of the elastic range during tests, and their purpose is rather to determine the functional properties of materials [12]. They are carried out practically exclusively on viscoelastic materials. Nevertheless, the results of such studies prove that for viscoelastic materials in particular, mechanical energy is dissipated during elastic deformation [13, 14].

This paper is the first of two parts of a study aimed at evaluating the impact of the strain rate of a plain weave GFRP laminate (adopted as the most characteristic type of reinforcement in laminates) in a static three-point bending test on the stress response of the material. Specifically, it is about showing whether and how the resistance of the material changes with increasing the deformation rate. The assessment was carried out only in the elastic range of deformation – it was considered that from the technical point of view this range is significant, and the obtained knowledge may have a significance in the application of the material and be a contribution to further research. The impact of the strain rate on the formation and development of failure (i.e. on the over-elastic range) is a separate issue, requires a different methodological approach and is not the subject of this study. It should be emphasized that the presented research is of a pioneering nature. As part of the first of two parts of the study, the assumptions and description of the method of conducting the experiments were included. The results and conclusions are discussed in the second part of the study, which is a separate publication.

## MATERIALS AND METHODS

### Non-destructive static bending tests

For the purpose of the study, a laminate based on the polyester resin ESTROMAL 14 (manufacturer ERG PUSTKÓW, Poland) was prepared, reinforced with 3 layers of plain weave glass fabric with an areal weight of 320 g/m$^2$ and the warp/weft mass ratio 1/1 (manufacturer KROSGLASS, Poland), stacked parallel one on one. The laminate was formed into a flat plate using the RTM pressure-vacuum method in a steel mold. A plate with both sides smooth was obtained. The volume fraction of the fibers (determined by the gravimetric method) was 49.5%. Three samples in the 0/90 direction and three samples in the 45/-45 direction were mechanically cut from the plate (Fig. 1a). Their dimensions are: 20 (± 0.2) x 80 (± 1) x 1.1 (± 0.05) mm. The samples were subjected to out-of-standard non-destructive static bending tests in a three-point system (Fig. 1b).

a)

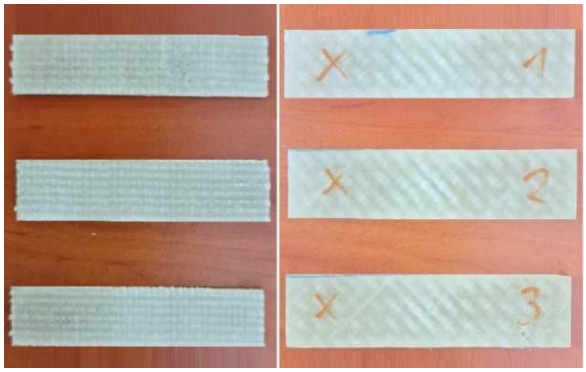


b)

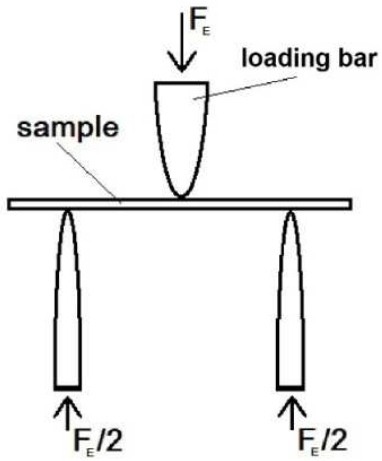


Fig. 1. Set of test samples (a) and diagram of applied bending method, with indication of loading bar (b): $F_E$ – load guaranteeing that material remains within elastic range of deformation

The adoption of the bending tests as the basis for the analysis was dictated by the simplicity, good repeatability of this type of tests and the lack of negative effects, e.g. slipping in the grips during stretching. Bending is often used in the analysis of the behavior of materials [15, 16]. Static bending tests were carried out using a ZWICK-ROEL 2.5 KN testing machine (Germany), the spacing of the supports was set at 77 mm. The test was non-standard, but it still was partially based on the guidelines of the PN-EN ISO 14125 standard. Non-destructive bending of each sample was carried out in the range of 0-2 mm; thus the maximum deformation obtained was below 0.23% and undoubtedly did not go beyond the elastic range (the limit of this range for the investigated type of composite is usually above 1.5%). The length of the samples guaranteed only a slight overhang beyond the supports. A large portion of the sample extending beyond the support may have some significance (cause additional inertia) at high deflection velocities. The deflection of 2 mm guaranteed the material to remain in an elastic state, but at the same time it guaranteed a sufficiently high strain of the material, effectively eliminating the significance of disturbances in the measurement results caused by stiffening of the loading system, friction of the sample on the supports, removal of the initial warping of the sample, etc.

 

The essence of the research was to bend the samples at different speeds. The tests were carried out for the bending speeds of 1, 10, 100 and 500 mm/min. After using the appropriate formula (developed on the basis of the PN-EN ISO 14125 standard), the appropriate maximum longitudinal normal strain rate of the material can be determined:

$$\varepsilon' = \frac{v \cdot 60 \cdot h}{L^2}$$

where: $\varepsilon'$ – strain rate (concerns deformation at the sample surface at the midspan, theoretically equal on the compression and tension sides of the bent beam), 1/s, $v$ – bending rate [mm/min], $h$ – height (thickness) of the sample [mm], $L$ – spacing of supporting bars [mm]. For the assumed geometric conditions, the applied bending rates corresponded to the material strain rates: $1.1 \cdot 10^{-3}$ 1/s, $1.1 \cdot 10^{-2}$ 1/s, $1.1 \cdot 10^{-1}$ 1/s and $5.6 \cdot 10^{-1}$ 1/s.

The measurement procedure included the following sequence of actions:

1) The sample was bent at a speed of 500 mm/min to a deflection of 2 mm. Then reverse bending was carried out automatically at a speed of –500 mm/min. The entire test was recorded – a hysteresis loop was drawn for each test.
2) After the test, the sample was turned upside down on supports and deflected in the opposite direction than during the actual test, to a position of 0.2 mm (such a value resulted in straightening of the sample, without overbending to the other side). Then, it was unloaded, removed from the supports and left for 24 hours. This action was aimed at fully relaxing the material.
3) After the assumed time had elapsed, the same sample was tested in a similar way at the deflection speeds of 100, 10 and 1 mm/min. For the speeds of 100 and 10 mm/min, no unloading of the sample was recorded (no hysteresis loop was drawn).
4) The actions described in points 1-3 were performed for each of the 6 prepared samples, divided into two series of 3 samples – the first in the 0/90 direction and the second in the 45/-45 direction (the warp/weft directions reflected).

The tests and relaxation of the samples were carried out at room temperature. The sets of load-deflection curves are shown in Appendix in Figures A1 and A2.

## Determination of modulus of elasticity at different strain rates

The elastic modulus was chosen as the main comparison criterion. As a rule, it is assumed that the modulus of elasticity is a constant property of the material, depending only on the temperature. Nonetheless, the above referred studies [1, 9] indicate that the strain rate should affect the value of the modulus.

Within the work, the method of determining the modulus of elasticity during bending was based on the guidelines of the PN-EN ISO 14125 standard. The procedure for each sample was as follows:

1) Two points were selected on the sample load-deflection curve, observing the rule that the first one was located just beyond the curve stabilization area at the initial loading section, and the second one was located near the end of the curve, i.e. 2 mm deflection.
2) For each point, the corresponding load and deflection were recorded – lists of the recorded values are given in Tables A1 and A2 in the Appendix.
3) Modulus of elasticity $E_g$ was determined according to the formula:

$$E_g = \frac{(F_2 - F_1) \cdot L^3}{4 \cdot b \cdot h^3 \cdot (f_2 - f_1)}$$

where: $F_2$ – load corresponding to the second assumed point in the curve [N], $F_1$ – load corresponding to the first assumed point in the curve [N], $f_2$ – deflection corresponding to the second assumed point in the curve [mm], $f_1$ – deflection corresponding to the first assumed point in the curve (mm), $L$ – spacing of supports [mm], $b$ – width of the sample [mm], $h$ – height of the sample [mm].

After determining the modulus for all three samples from a given measurement series (corresponding to one of the four deflection velocities), the mean value was taken and the measurement error was determined. The results of the obtained moduli are graphically shown in Figures A3 and A4 in the Appendix.

## Determination of energy dissipated in load-unload cycle

In order to extend the assessment of the behavior of the materials tested at different deflection velocities in the elastic range, the energy dissipated in the load-unload cycle was determined. The bending tests were carried out according to the sequence described above, for the bending (and reverse bending) speeds of 1 and 500 mm/min (two extreme cases). The method of determining the energy from the acquired curves was based on the precise assessment of the surface area between the loading and unloading curves – an example of the surface area for the calculations is shown in Figure 2.

The presence of an evident hysteresis loop proves the non-linearity of the deformations in the analyzed range. The complete set of obtained hysteresis loops is shown in Figures A5 and A6 in the Appendix. The significance of the observed behavior and its dependence on the loading rate of the samples are discussed in the second part of the study.

 

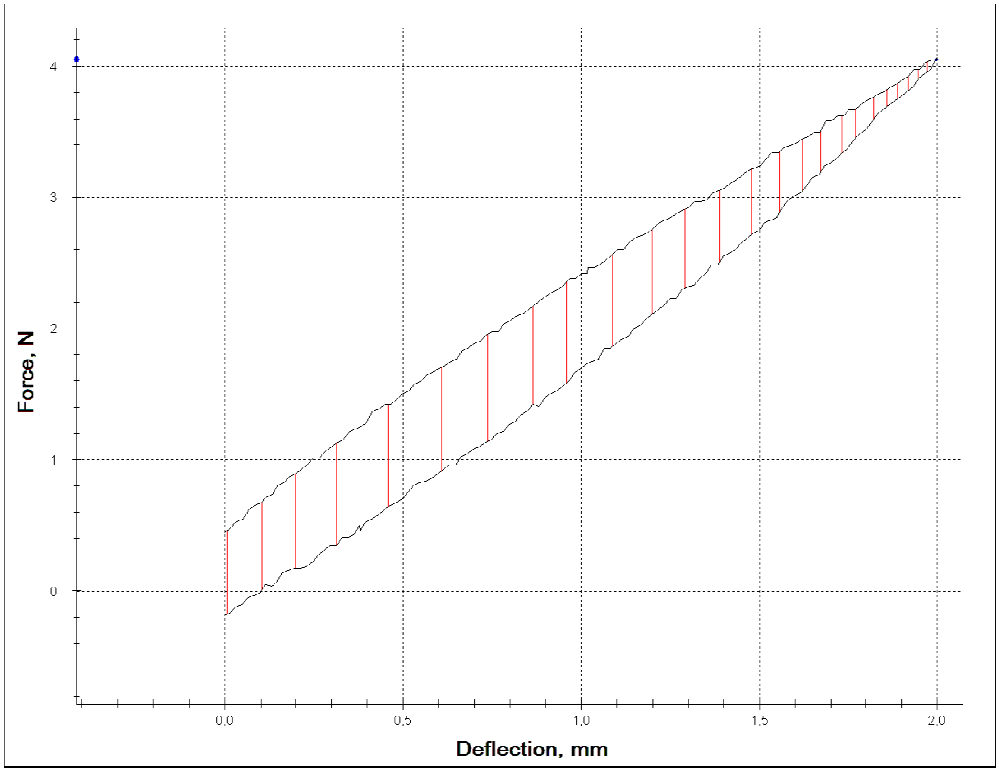


Fig. 2. Area of loop determined by load-deflection curves of example sample at speed of 1 mm/min – surface area of this area corresponds to mechanical work energy utilized by tested sample in one load-unload cycle

## Acknowledgements

*The study was funded by the Silesian University of Technology as a part of statutory research, projects No. BK-209/RM3/2022 and BK/RM3/2023.*

## REFERENCES

[1] Jurczak W., Wpływ prędkości odkształcenia na właściwości mechaniczne stopu AlZn5Mg2CrZr i stali kadłubowej kat. A, Zeszyty Naukowe Akademii Marynarki Wojennej 2007, XLVIII, 171(4), 37-47.

[2] Pawlicki J., Rodak K., Płachta A., Plastyczność wybranych materiałów metalicznych w warunkach dynamicznego odkształcania, Zeszyty Naukowe Politechniki Śląskiej 2014, Seria Transport, 83, 173-182.

[3] Leszczyńska B., Richert M., Wpływ dużych prędkości odkształcenia na właściwości mechaniczne i rozdrobnienie struktury w aluminium i miedzi, Rudy i Metale Nieżelazne 2005, 50, 10-11, 586-590.

[4] Rabek J.F., Współczesna wiedza o polimerach. Tom 1, WN PWN, Warszawa 2017.

[5] Hyla I., Tworzywa sztuczne, Wydawnictwo Politechniki Śląskiej, Gliwice 2004.

[6] Pielichowski J., Puszyński A., Chemia polimerów, FOSZE, Rzeszów 2012.

[7] Hearn E.J., Mechanics of Materials 2: The Mechanics of Elastic and Plastic Deformation of Solids and Structural Materials. Butterworth-Heinemann, Oxford, UK, 1997.

[8] Fengqiang Gong, Hao Ye, Yong Luo, The effect of high loading rate on the behaviour and mechanical properties of coal-rock combined body, Shock and Vibration 2018, Article nr 4374530, DOI: 10.1155/2018/4374530.

[9] Wiesner C.S., MacGillivray H., Loading rate effects on tensile properties and fracture toughness of steel, Proceedings of The 1999 TAGSI Seminar on Fracture, Plastic Flow and Structural Integrity, Cambridge, UK, 29 April 1999.

[10] Klasztorny M., Nycz D.B., Modelling of linear elasticity and viscoelasticity of thermosets and unidirectional glass fibre-reinforced thermoset-matrix composites – Part 1: Theory of Modeling, Composites Theory and Practice 2022, 22(1), 3-15.

[11] Klasztorny M., Nycz D.B., Modelling of linear elasticity and viscoelasticity of thermosets and unidirectional glass fibre-reinforced thermoset-matrix composites – Part 2: Homogenization and Numerical Analysis, Composites Theory and Practice 2022, 22(1), 25-39.

[12] Gnanaseelan M., Trommer K., Gude M., Stanik R., Przybyszewski B., Kozera R., Boczkowska A., Effect of strain on heating characteristics of silicone/cnt composites, Materials 2021, 14(16), 4528.

[13] Kurzeja L., Szeluga U., Grishchuk S., Właściwości wiskoelastyczne i mechaniczne epoksydowanego nowolaku o-krezolowego, Zeszyty Naukowe Chemia Politechnika Śląska 1999, 311-314.

[14] Pusz S., Szeluga U., Nagel B., Czajkowska S., Galina H., Strzezik J., The influence of structural order of anthracite fillers on the curing behavior, morphology, and dynamic mechanical thermal properties of epoxy composites, Polymer Composites 2015, 36(2), 336-347.

[15] Bellini C., Borrelli R., Di Caprio F.D., Di Cocco V., Francitti S., Iacoviello F., Mocanu L.P., Sorrentino L., Hybrid structures in Titanium-Lattice/FRP: Effect of skins material on bending characteristics, Procedia Structural Integrity 2022, 41, 3-8.

[16] Bellini C., Borrelli R., Di Cocco V., Franchitti S., Iacoviello F., Sorrentino L., Titanium lattice structures manufactured by EBM process: Effect of skin material on bending characteristics, Engineering Fracture Mechanics 2022, (260), 108180.

 

## APPENDIX

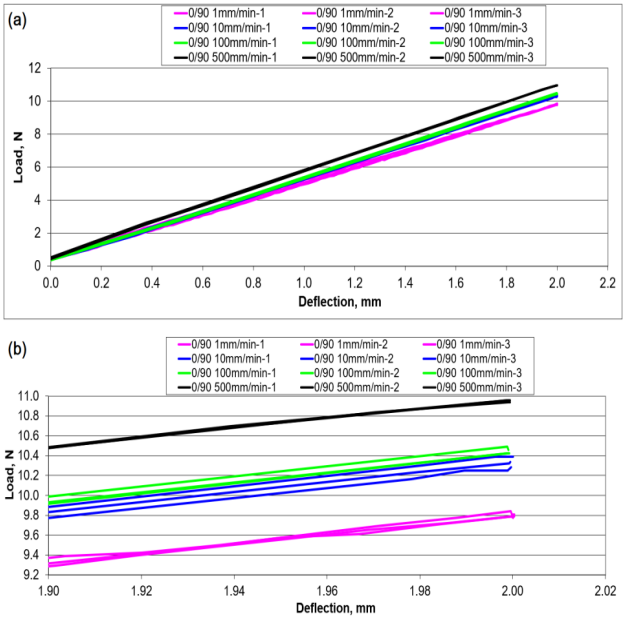


Fig. A1. Original bending curves of samples at different loading rates – samples in 0/90 direction: a) full course of curves, b) zoom of curves, where differences caused by different loading rates and actual spread of curves are clearly visible

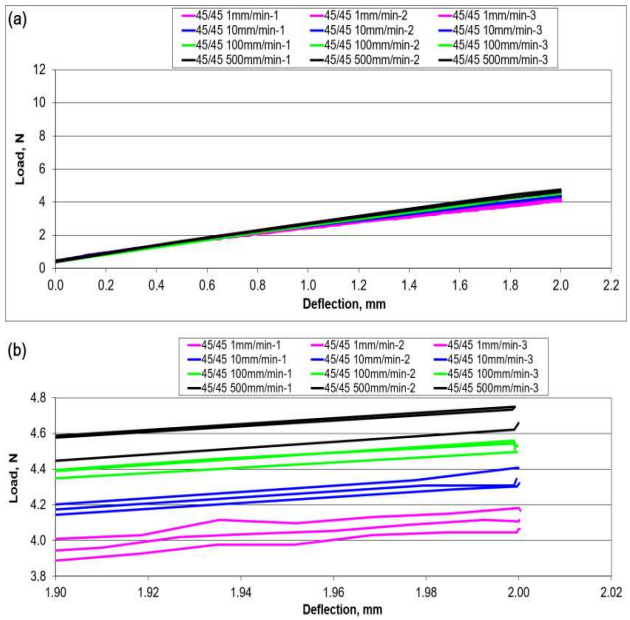


Fig. A2. Original bending curves of samples at different loading rates – samples in 45/-45 direction: a) full course of curves, b) zoom of curves, where differences caused by different loading rates and actual spread of curves are clearly visible

TABLE A1. **Calculations of elastic modulus $R_g$ – samples 0/90**

| **Sample** | **point 1 [N]** | **point 2 [N]** | **point 1 [mm]** | **point 2 [mm]** | **Modulus $R_g$ [MPa]** |
|---|---|---|---|---|---|
| 1 mm/min – sample 1 | 2.79 | 9.77 | 0.52 | 2.00 | 9948 |
| 1 mm/min – sample 2 | 2.96 | 9.81 | 0.52 | 2.00 | 9748 |
| 1 mm/min – sample 3 | 2.59 | 9.81 | 0.50 | 2.00 | 10168 |
| | | | | Mean: | 9955 |
| | | | | Std. deviation: | 210 |
| | | | | | |
| **Sample** | **point 1 [N]** | **point 2 [N]** | **point 1 [mm]** | **point 2 [mm]** | **Modulus $R_g$ [MPa]** |
| 10 mm/min – sample 1 | 3.43 | 9.58 | 0.64 | 1.89 | 10462 |
| 10 mm/min – sample 2 | 3.55 | 10.28 | 0.64 | 2.00 | 10508 |
| 10 mm/min – sample 3 | 3.60 | 10.39 | 0.65 | 2.00 | 10616 |
| | | | | Mean: | 10529 |
| | | | | Std. deviation: | 79 |
| | | | | | |
| **Sample** | **point 1 [N]** | **point 2 [N]** | **point 1 [mm]** | **point 2 [mm]** | **Modulus $R_g$ [MPa]** |
| 100 mm/min – sample 1 | 4.53 | 10.46 | 0.83 | 2.00 | 10739 |
| 100 mm/min – sample 2 | 4.49 | 10.42 | 0.84 | 2.00 | 10858 |
| 100 mm/min – sample 3 | 4.53 | 10.42 | 0.84 | 2.00 | 10797 |
| | | | | Mean: | 10798 |
| | | | | Std. deviation: | 59 |
| | | | | | |
| **Sample** | **point 1 [N]** | **point 2 [N]** | **point 1 [mm]** | **point 2 [mm]** | **Modulus $R_g$ [MPa]** |
| 500 mm/min – sample 1 | 4.70 | 10.94 | 0.78 | 2.00 | 10824 |
| 500 mm/min – sample 2 | 4.49 | 10.96 | 0.76 | 2.00 | 10988 |
| 500 mm/min – sample 3 | 4.51 | 10.94 | 0.77 | 2.00 | 11039 |
| | | | | Mean: | 10950 |
| | | | | Std. deviation: | 112 |

 

TABLE A2. **Calculations of elastic modulus $R_g$ – samples 45/-45**

| Sample | point 1 [N] | point 2 [N] | point 1 [mm] | point 2 [mm] | Modulus $R_g$ [MPa] |
|---|---|---|---|---|---|
| 1 mm/min – sample 1 | 1.53 | 4.06 | 0.52 | 2.00 | 3615 |
| 1 mm/min – sample 2 | 1.59 | 4.17 | 0.52 | 2.00 | 3662 |
| 1 mm/min – sample 3 | 1.56 | 4.11 | 0.52 | 2.00 | 3639 |
| | | | | Mean: | 3638 |
| | | | | Std. deviation: | 23 |
| | | | | | |
| **Sample** | **point 1 [N]** | **point 2 [N]** | **point 1 [mm]** | **point 2 [mm]** | **Modulus $R_g$ [MPa]** |
| 10 mm/min – sample 1 | 1.87 | 4.70 | 0.65 | 2.00 | 4427 |
| 10 mm/min – sample 2 | 1.95 | 4.41 | 0.64 | 2.00 | 3823 |
| 10 mm/min – sample 3 | 1.85 | 4.32 | 0.65 | 2.00 | 3863 |
| | | | | Mean: | 4038 |
| | | | | Std. deviation: | 338 |
| | | | | | |
| **Sample** | **point 1 [N]** | **point 2 [N]** | **point 1 [mm]** | **point 2 [mm]** | **Modulus $R_g$ [MPa]** |
| 100 mm/min – sample 1 | 2.30 | 4.50 | 0.87 | 2.00 | 4117 |
| 100 mm/min – sample 2 | 2.43 | 4.53 | 0.88 | 2.00 | 3962 |
| 100 mm/min – sample 3 | 2.27 | 4.51 | 0.86 | 2.00 | 4145 |
| | | | | Mean: | 4075 |
| | | | | Std. deviation: | 99 |
| | | | | | |
| **Sample** | **point 1 [N]** | **point 2 [N]** | **point 1 [mm]** | **point 2 [mm]** | **Modulus $R_g$ [MPa]** |
| 500 mm/min – sample 1 | 2.61 | 4.66 | 0.98 | 2.00 | 4245 |
| 500 mm/min – sample 2 | 2.45 | 4.75 | 0.87 | 2.00 | 4300 |
| 500 mm/min – sample 3 | 2.45 | 4.75 | 0.87 | 2.00 | 4304 |
| | | | | Mean: | 4283 |
| | | | | Std. deviation: | 33 |

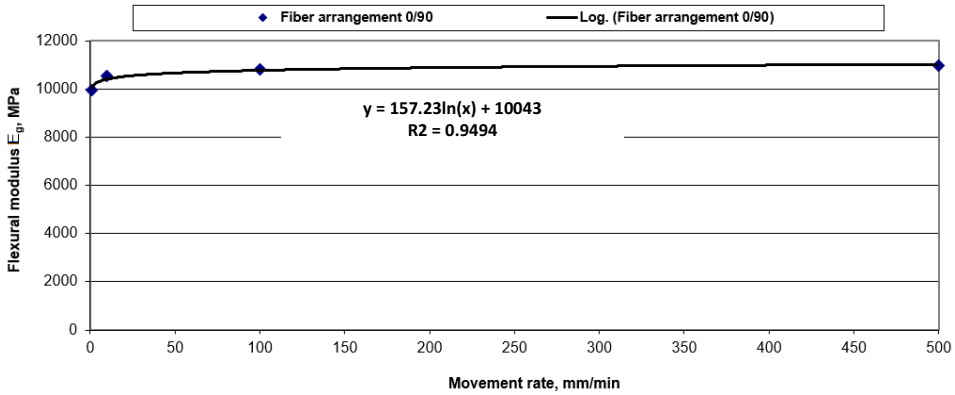


Fig. A3. Elastic modulus vs. loading bar movement rate (during three-point bending) – samples 0/90

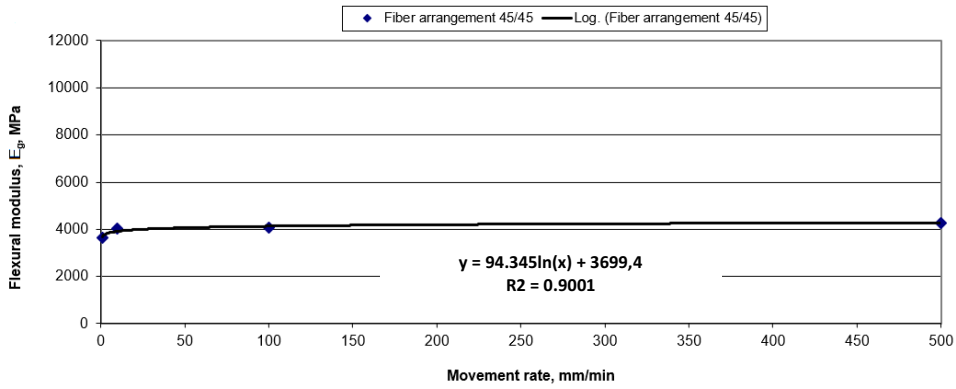


Fig. A4. Elastic modulus vs. loading bar movement rate (during three-point bending) – samples 45/-45

 

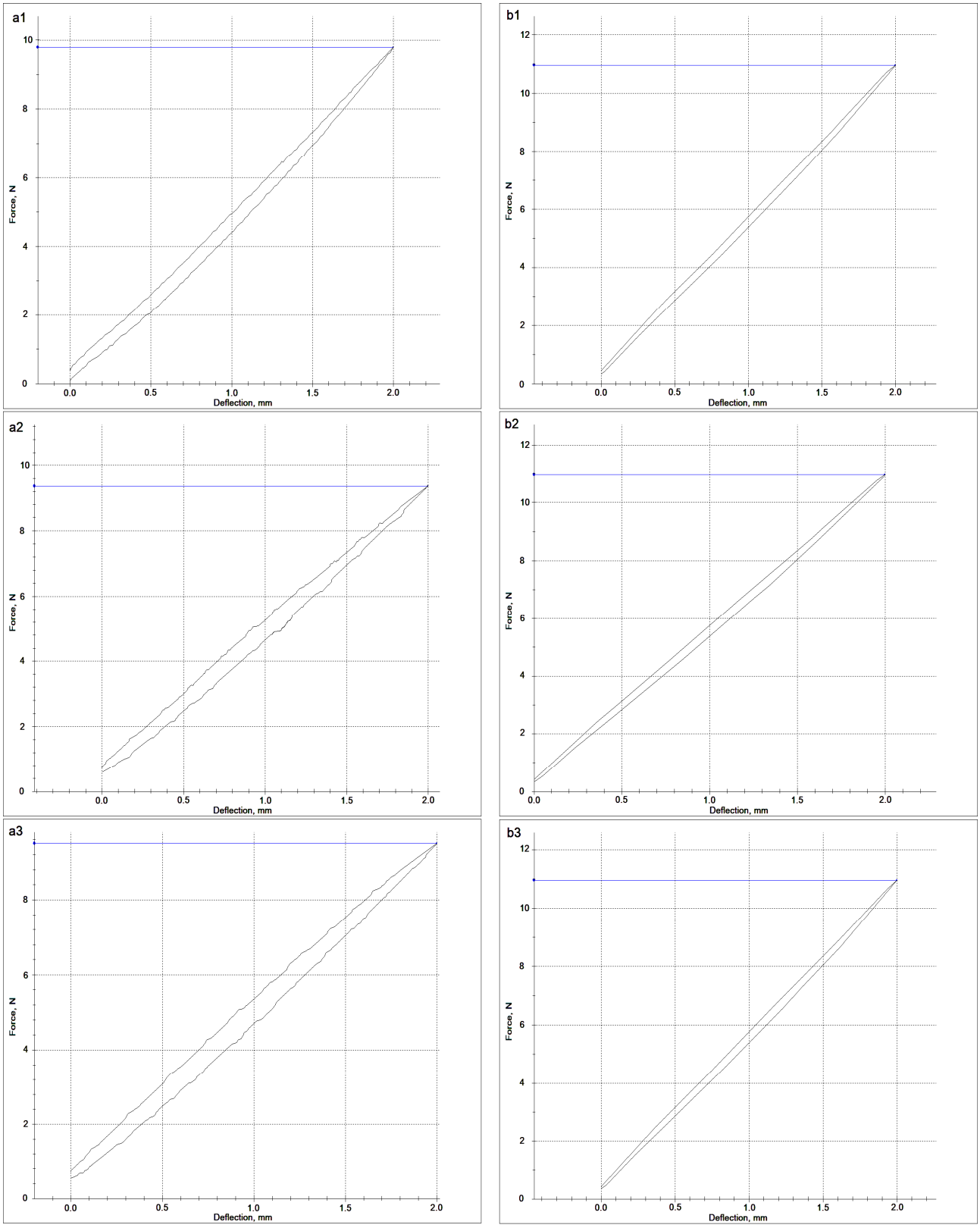


Fig. A5. Mechanical energy of load-unload cycle (static three-point bending) – samples 0/90

 

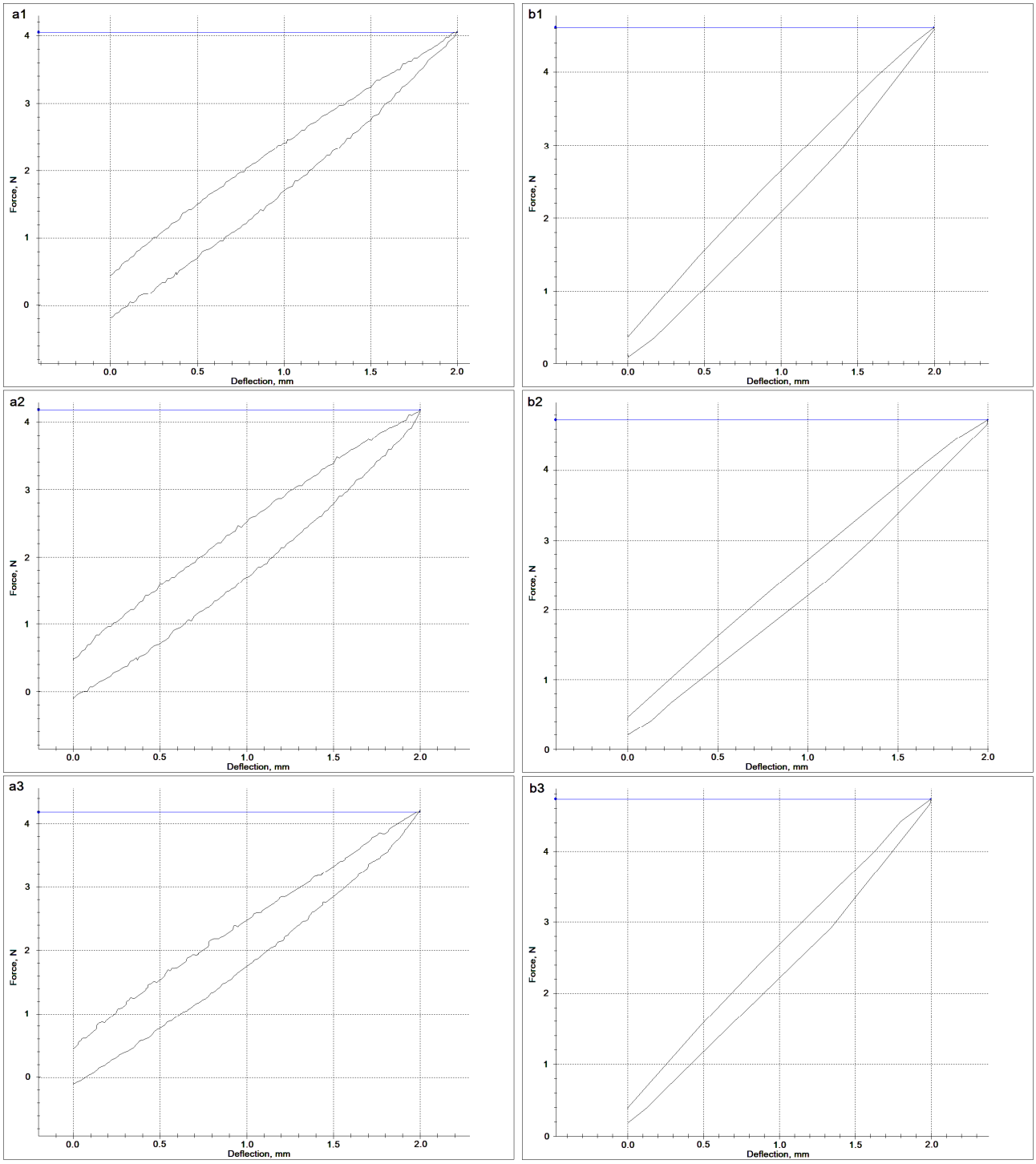


Fig. A6. Mechanical energy of load-unload cycle (static 3-point bending) – samples 45/-45

 